

Variation of Threshold Field in Field Induced Fabrication of Au Nanodots on Ultrathin in-situ Grown Silicon Oxide.

Jeong Young Park^{1,3, a)}, R. J. Phaneuf^{2,3}, and E. D. Williams^{1,3}

¹ Department of Physics, University of Maryland College Park, Maryland 20742

² Department of Materials Science and Engineering, University of Maryland College Park, Maryland 20742

³ Laboratory for Physical Sciences, College Park, Maryland 20740

We report on the variation of threshold field with oxide thickness for field evaporation of Au nanodots onto ultrathin oxide layers on Si(100). Au dots of 1 –10 nm diameter were fabricated on an in-situ oxidized Si(100) substrate by the application of a voltage pulse between an Au coated STM tip and the sample. Under feedback-controlled tunneling conditions ($V_s = 2$ V, $I_t = 3$ nA), the voltage required for field-deposition increased roughly linearly from 5.8 to 11 volts as average oxide thickness increased from zero to 8 Å. This corresponds to a change in the threshold field of about 0.3 V/Å, which is roughly consistent with a calculation based on shielding of the image charge by the intervening oxide layer.

Keywords : Scanning Tunneling Microscopy, Au dot, Silicon oxide, Field evaporation, Threshold field, Field induced fabrication.

^{a)} Corresponding author. Fax: +1 301 935 6723, e-mail address: jpark@lps.umd.edu

The fabrication and modification of nanometer scale structure with Scanning Probe Microscopy (SPM) have attracted much attention during the last decade because of potential application in the study of quantum transport, single electron tunneling (SET) devices, and fabrication of novel nanoelectronic structures. Various techniques for nanoscale modification have been demonstrated [1-3]. Of these, direct transfer of material by field evaporation from a Scanning Tunneling Microscopy (STM) tip, first demonstrated by Mamin et al. [4], is particularly interesting because it allows characterization as well as fabrication of nanostructure.

Subsequent studies have concentrated on the mechanisms of nanostructure formation including direct transfer of various materials by field evaporation [5-8]. Still other studies have characterized the threshold for field evaporation from STM, Atomic Force Microscopy (AFM), and Field Ion Microscopy (FIM) tips onto substrates with or without an intervening oxide or in the absence of a substrate at all [4-13]. These measurements confirm that the threshold field increases as the image potential associated with the substrate decreases, in qualitative agreement with models proposed by Tsong and Miskovsky for field evaporation to a conducting surface [14,15].

In this work, we measured the variation of the threshold voltage with oxide thickness for fabrication of Au nanodots on oxidized Si(100) in the ultrathin oxide regime. We compare our results with predictions of a simple continuum model in which the screening of the image potential by the oxide is explicitly included.

The experiment was performed with a commercial STM (Park Scientific Instruments Autoprobe VP) operated in a vacuum chamber with a base pressure of $1.0 \times$

10^{-10} torr. Tungsten STM tips were first electrochemically etched, then Au coated by thermal evaporation in a separate chamber. The thickness of Au was measured with a quartz crystal monitor and checked by comparing SEM (Scanning Electron Microscopy) images before and after coating. Typical thicknesses were approximately 40 nm.

The silicon samples were n-type (20x10x0.5 mm, P-doped, 2-3 $\Omega\cdot\text{cm}$ resistivity, (100) orientation $\pm 0.1^\circ$). These were chemically etched using the Shiraki method [16], then installed in vacuum and heated to approximately 1250 $^\circ\text{C}$ using electron bombardment. After cooling the sample at a rate of approximately 2 $^\circ\text{C}/\text{s}$ [17], STM images measured with a Au coated tip showed a (2x1) dimer row reconstruction structure indicating an atomically sharp triplet. Due to the nonreactive nature of the Au coating, the tunneling characteristics are quite stable. Surfaces were oxidized by exposing to pure O_2 gas at a pressure of 2.0×10^{-7} torr at a temperature of 540 $^\circ\text{C}$. A published calibration of the sticking coefficient of oxygen on Si(100) as a function of temperature was used to estimate the thickness of oxide [18,19].

For the nanodot fabrication, we applied voltage pulses to the sample while monitoring the tunneling current. The pulse height was varied between -10 V and $+10$ V. The pulse width was varied from 0.1 ms to 100 ms. The tip height was determined using a sample voltage and tunneling current of 2V and 3nA, respectively. During application of the pulse, the feedback was switched off to keep the tip-sample distance nearly constant.

Figure 1(a) shows an STM image of a Si(100) surface after desorbing the oxide and cooling to near room temperature. The characteristic 2x1 dimer row reconstruction structure with missing dimer defects can be seen in this image. The areal density of the

defects is less than 3 %. Figure 1(b) shows an image of the same silicon surface after oxidation (5 L O₂ at 540 °C, ~0.2 ML) and application of a – 8 V, 10 ms pulse to form a Au dot. Atomically resolved features are visible in Fig 1(b), indicating that the tip regenerates after dot formation. The typical diameter of dots formed is between 3~10 nm with a height between 0.4 ~ 2 nm. The sizes are strongly dependent on the height and polarity of the pulse. The voltage pulses of tip-positive polarity give rise to the transfer of Au dots with larger size (> 20 nm) [10].

Figures 2 (a) –(d) show the determination of the threshold voltage, in this case for an oxide of coverage 2.2 ML. Before acquiring each image, we applied 10 voltage pulses with heights of - 6 V (Fig 2(a)), - 7.5 V (Fig 2(b)), and - 9 V (Fig 2(c)) and a duration of 100 ms to the tip, then imaged and counted the total number of dots formed. Following the convention adopted by Mamin et al. and Chang et al. [4,5], the threshold voltage of field evaporation is defined as the voltage where the probability of making features is saturated. From the plot of probability of dot formation (e.g. the ratio of number of dots formed to the number of voltage pulses) as shown in Fig. 2(d), the threshold voltage in this case is approximately – 8.2 V. We repeated this procedure for surfaces with different thickness of oxide, and found that the threshold voltage (V_{th}) increases approximately linearly with oxide thickness as shown in Fig. 3(a). To compare with theory, it is necessary to extract the threshold field, which requires knowledge of the tip sample separation. Based upon a Fowler-Nordheim analysis of the current-voltage characteristic, we estimate the tip sample separation for the clean surface to be 6 Å for our initial sample voltage of 2 V, and tunneling current of 3 nA.

The extracted threshold field for field evaporation is given by

$$F_{TH} = \frac{V_{TH}}{d_o + \frac{\epsilon_0}{\epsilon_{ox}} t_{ox}} \quad (1)$$

Where ϵ_{ox} and ϵ_o are the oxide dielectric constant of oxide and vacuum respectively, t_{ox} is the oxide thickness, V_{TH} is the threshold voltage difference in oxide and vacuum, and $d_o(t_{ox})$ is separation between the tip and the top of the oxide (see Fig 3(a)). We use the bulk value of 3.9 for the oxide dielectric constant, ignoring the possibility of a variation in this with thickness for ultrathin oxides. It should be noted that d_o is dependent on the oxide thickness t_{ox} since the feedback circuit adjusts the tip height to maintain the same setpoint current. This dependence was calibrated by measuring the height difference between the oxide and areas of bare silicon in STM images of partially oxidized silicon surfaces, and using the known oxide thickness vs. coverage[18,19]. In the case of the chemically prepared Shiraki oxide, d_o was estimated by fitting to the tunneling equation. The threshold field determined by Equation (1) [F_{TH} in Fig 3(b)] increases nearly linearly with oxide thickness from 0.96 V/Å for the atomically clean surface to 1.2 V/Å for 3.6 Å oxide. The threshold voltage and field for a chemically prepared Shiraki oxide of thickness 8 Å were also determined, and found to be 11 V and 1.3 V/Å respectively.

The threshold field for negative Au ions has previously been studied for various configurations. Mamin et al. measured 0.4 V/Å for a Au surface in air with a Au tip [4]. Chang et al. measured 0.6 V/Å for a Au surface in UHV [5]. Koyanagi et al. measured a

larger value, 1.3 V/Å for evaporation onto a Si surface through a thick (17-100 Å) oxide [11]. Tsong et al. measured an even larger value, 3.5 V/Å for an isolated Au FIM tip [13]. The overall trend agrees with expectations based upon the lowering of the energy barrier due to the image charge[see Fig. 3(a)], which is absent in the isolated tip case. The increased threshold field with oxide thickness shown in Fig. 3 is also in qualitatively agreement with such an effect.

To make a quantitative comparison, we calculate the threshold field based on the charge exchange model for field evaporation including the screened image potential. For an oxidized surface, Koyanagi et al. have proposed the following variation for the threshold field on the oxide thickness t_{ox} derived from an equation given by Tsong [11,14].

$$F_{CEM} = \frac{1}{nr_0} \left(\Lambda + n\phi - \sum A_i - \frac{3.6n^2}{r_0} - \frac{3.6n^2}{d_0(t_{ox}) - r_0} \left(\frac{\epsilon_{ox} - 1}{\epsilon_{ox} + 1} \right) - \frac{3.6n^2}{t_{ox}\epsilon_{ox} + d_0(t_{ox})} - Q_{in} \right) \quad (2)$$

Where Λ is binding energy of the tip atom, $\sum A_i$ is the total electron affinity of the tip atom to the n - charge state, ϕ is the work function of the tip, and r_0 is the effective atomic diameter of tip atom. The fifth and sixth terms are a first approximation of the image potential for the oxide, and the conducting Si surface. Q_{in} is the activation energy for field evaporation. We compare our measured values with this simple model, using $\Lambda=3.78$ eV, $A_1=2.31$ eV, $r_0=1.44$ Å, and $Q_{in}=0.84$ eV, [14] and taking $d_0=6$ Å for clean silicon surface. The values of the sample tip separation ($d_0(t_{ox})$) and oxide thickness (t_{ox}) listed in Table 1 were used to calculate the thickness-dependent variation from Eq. 2. This model assumes a continuous value for t , which is not obviously correct for the ultrathin oxide

regime. It also neglects the effect of trapped charge due to oxide-silicon interface states, and the depletion layer. Because our measured IV profiles indicate the Metal Insulator Semiconductor (MIS) junction formed by the tip, tunneling gap and oxide, and Si surface to be in inversion for the measured threshold voltages, this last effect is not likely to be significant. Figure 3(b) shows the calculated variation in the field, as well as that extracted from the measured threshold voltage, with oxide thickness. The average value over our range of measurement is nearly same in both cases, and both the model- and the data-derived fields show an increase with oxide thickness. However, while the calculated curve based upon the model saturates by approximately 3 Å of oxide thickness, the measured values are approximately linear. We note however that uncertainties associated with a small number of measurement to derive the threshold fields do not allow us to convincingly exclude saturation.

A limitation of the model concerns the layer-by-layer growth of oxide on Si(100), suggesting a discrete model rather than continuum model. We have also calculated the average field based upon a layer by layer growth model and find improved (e. g. a more nearly linear variation) agreement near zero coverage, but still find a saturation at approximately 3 Å.

In summary, we have measured the variation of the threshold for field evaporation with oxide coverage for ultrathin oxide layers. Under feedback tunneling conditions, the threshold voltage increases roughly linearly with oxide thickness from zero to 8 Å. The corresponding threshold field increases monotonically by approximately 0.3 V/Å over the same range, in rough agreement with predicted behavior for a simple continuum charge exchange model including screening of the image potential by the oxide. The

detailed shape of the predicted thickness-variation may be modified by details of the growth model and chemical state of the ultra-thin oxide.

Acknowledgement

This work has been supported by the Laboratory for Physical Sciences and in part by the University of Maryland-NSF-MRSEC (NSF-DMR-00-80008)

References

1. J. Stroschio, and D. Eigler, *Science* **254**, 1318 (1991).
2. I. –W. Lyo, and P. Avouris, *Science* **253**, 173 (1991).
3. A. Kobayashi, F. Grey, R. S. Williams, and M. Aono, *Science* **259**, 1724 (1993).
4. H. J. Mamin, P. H. Guethner, and D. Rugar, *Phys. Rev. Lett.* **65**, 2418 (1990).
5. C. S. Chang, W. B. Su, and T. T. Tsong, *Phys. Rev. Lett.* **72**, 574 (1994).
6. G. S. Hsiao, R. M. Penner, and J. Kingsley, *Appl. Phys. Lett.* **64**, 1350 (1994).
7. K. Bessho, and S. Hashimoto, *Appl. Phys. Lett.* **65**, 2142 (1994).
8. X. Hu, and P. von Blanckenhagen, *Appl. Phys. A* **66**, S707 (1998).
9. Ch. Mascher and B. Damaschke, *J. Appl. Phys.* **75**, 5438 (1994).
10. D. Fujita, Q. Jiang, and H. Nejoh, *J. Vac. Sci. Technol. B* **14**, 3413 (1996).
11. H. Koyanagi, S. Hosaka, R. Imura, and M. Shirai, *Appl. Phys. Lett.* **67**, 2609 (1995).
12. S. Hosaka, H. Koyanagi, A. Kikukawa, W. Maruyama, and R. Imura, *J. Vac. Sci. Technol. B* **12**, 1872 (1994).
13. T. T. Tsong, *Surf. Sci.* **70**, 211 (1978).
14. T. T. Tsong, *Phys. Rev. B* **44**, 13703 (1991).
15. N. M. Miskovsky and T. T. Tsong, *Phys. Rev. B* **46**, 2640 (1992).
16. A. Ishizaki and Y. Shiraki, *J. Electrochem. Soc.* **133**, 666 (1986).
17. See, for example B. S. Swartzentruber, Y. –W. Mo, M. B. Webb, and M. G. Lagally, *J. Vac. Sci. Technol. A* **7** 2901 (1989).
18. T. Engel, *Surf. Sci. Rep.* **18**, 91 (1993).
19. J. Westermann, H. Nienhaus, and W. Mönch, *Surf. Sci.* **311**, 101 (1994).

Table I. The values of oxide thickness and corresponding tip sample separation.

t_{ox} (Å)	$d_0(t_{\text{ox}})$ (Å)
0	6.0
0.4	6.0
1.3	5.9
2.0	5.8
2.6	5.7
3.6	5.6
8 (Shiraki oxide)	6.5

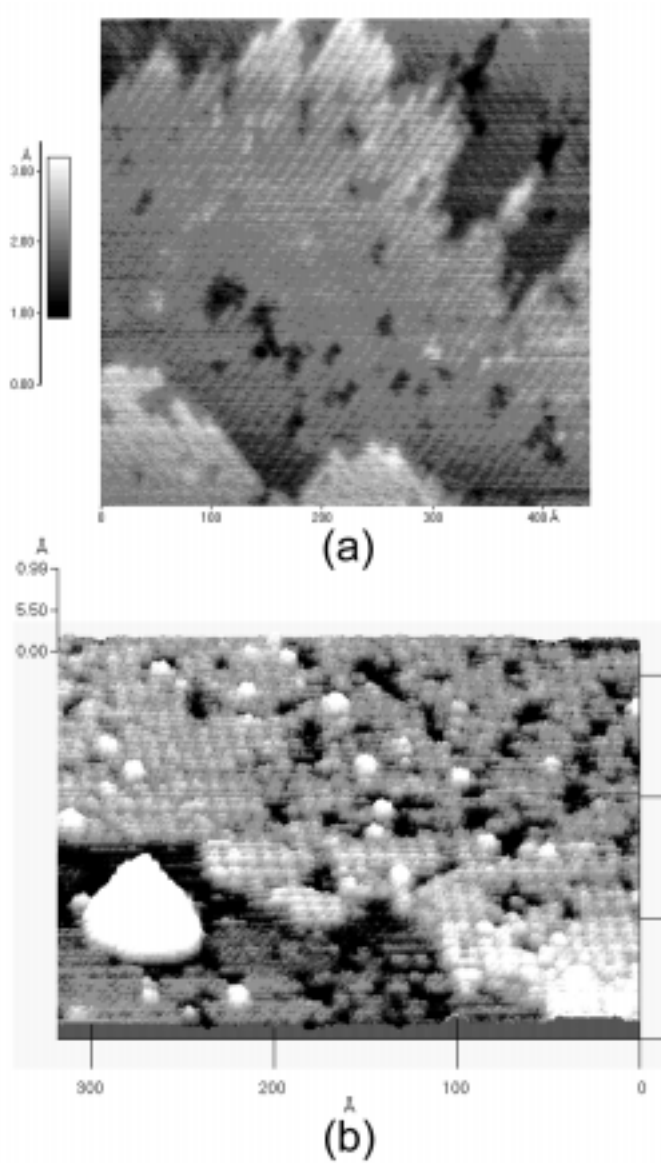


Figure 1(a) STM image of a Si (100) dimer row reconstructed surface taken with a Au coated tip. The density of defect is less than 3 %. (b) Au dot on a partially oxidized silicon surface whose size is 7 nm and height is 10 Å. The tip regenerates and shows an atomic resolution image after making Au dots.

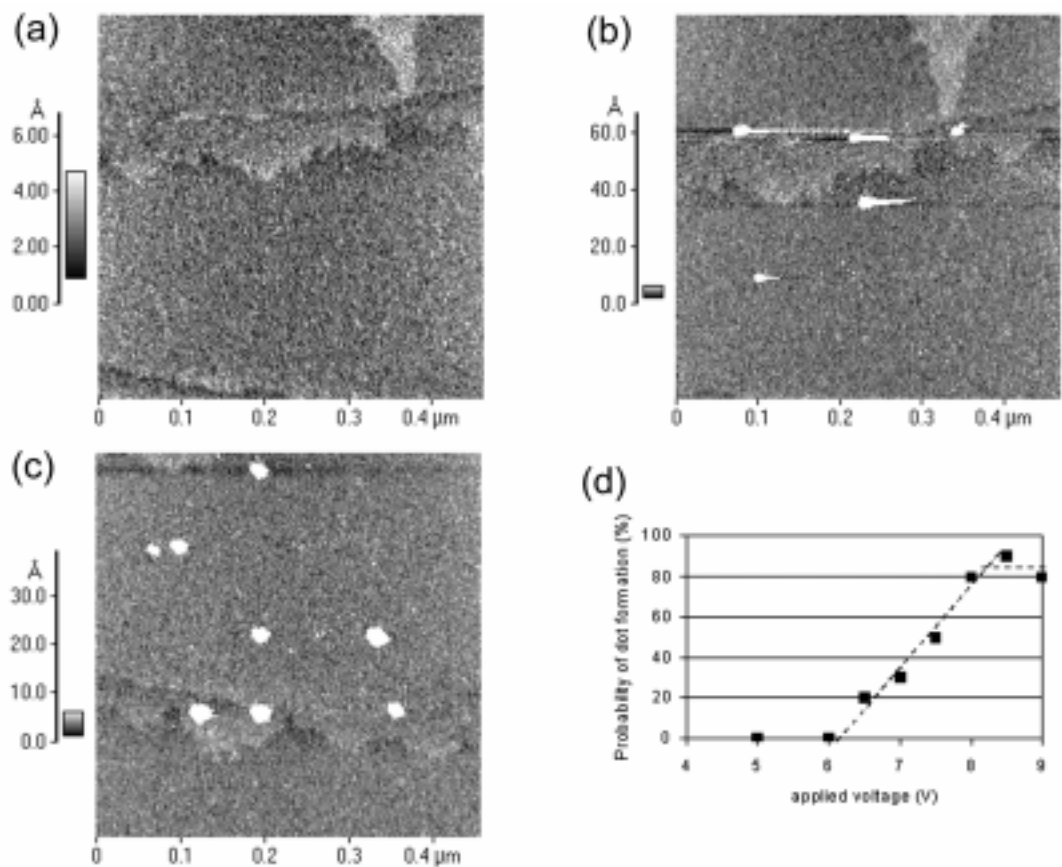


Figure 2. (a)-(c) STM images of oxidized Si (100) after application of multiple voltage pulses between sample and tip. Silicon oxide coverage is 2.2 ML. For these images 10 voltage pulses were applied with heights of -6 V(a), -7.5 V (b), and -9 V (c) to the tip. (d) The probability of dot formations as a function of applied voltage. The threshold voltage is determined to be -8.2 V.

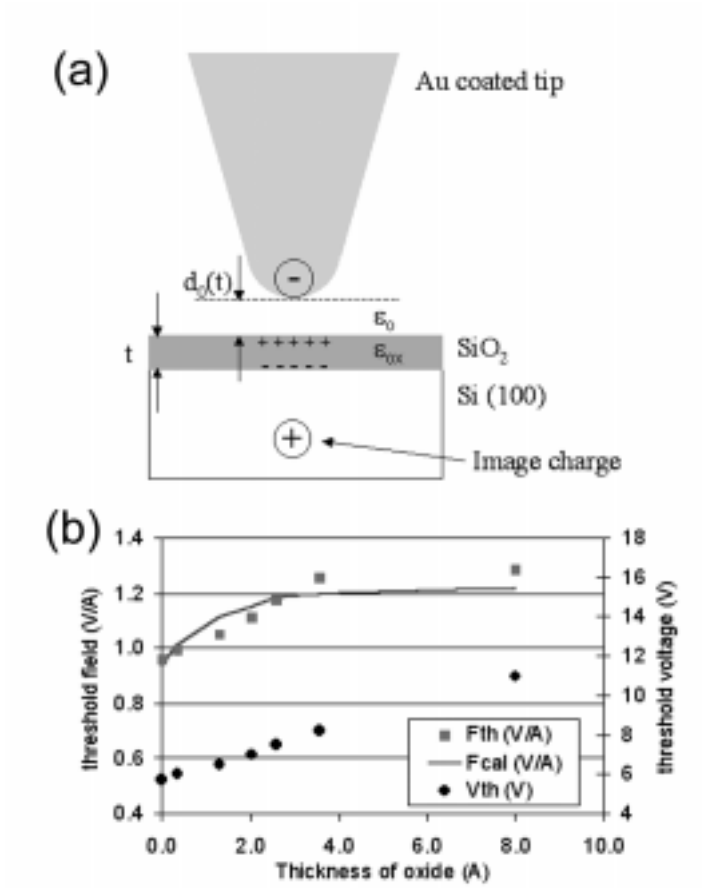


Figure 3 (a) Schematic showing the screening of the attractive force between image charges by oxide. (b) Measured threshold voltage (V_{TH}), corresponding threshold field (F_{TH}), and calculated threshold field (F_{CAL}) versus the oxide thickness.